Journal of ELECTRONIC MATERIALS, Vol. 39, No. 11, 2010
DOI: 10.1007/s11664-010-1346-6
© 2010 TMS

Study of Interfacial Reactions Between Sn(Cu) Solders and Ni-Co Alloy Layers

K.C. HUANG,[1] F.S. SHIEU,[1] T.S. HUANG,[2,3] C.T. LU,[2] C.W. CHEN,[2] H.W. TSENG,[2] S.L. CHENG,[2] and C.Y. LIU[2]

1.—Department of Materials Science and Engineering, National Chung-Hsing University, Taichung, Taiwan. 2.—Department of Chemical Engineering and Materials Engineering, National Central University, Chung-Li City, Taiwan. 3.—e-mail: birdsong1114@yahoo.com.tw

The interfacial reactions between electroplated Ni-*y*Co alloy layers and Sn(Cu) solders at 250°C are studied. For pure Co layers, $CoSn_3$ is the only interfacial compound phase formed at the Sn(Cu)/Co interfaces regardless of the Cu concentration. Also, the addition of Cu to Sn(Cu) solders has no obvious influence on the $CoSn_3$ compound growth at the Sn(Cu)/Co interfaces. For Ni-63Co layers, $(Co,Ni,Cu)Sn_3$ is the only interfacial compound phase formed at the Sn(Cu)/Ni-63Co interfaces. Unlike in the pure Co layer cases, the Cu additives in the Sn(Cu) solders clearly suppress the growth rate of the interfacial $(Co,Ni,Cu)Sn_3$ compound layer. For Ni-20Co layers, the interfacial compound formation at the Sn(Cu)/Ni-20Co interfaces depends on the Cu content in the Sn(Cu) solders and the reflow time. In the case of high Cu content in the Sn(Cu) solders (Sn-0.7Cu and Sn-1.2Cu), an additional needle-like interfacial $(Ni_x,Co_y,Cu_{1-x-y})_3Sn_4$ phase forms above the continuous $(Ni_x,Cu_y,Co_{1-x-y})Sn_2$ compound layer. The Ni content in the Ni-*y*Co layer can indeed reduce the interfacial compound formation at the Sn(Cu)/Ni-*y*Co interfaces. With pure Sn solders, the thickness of the compound layer monotonically decreases with the Ni content in the Ni-*y*Co layer. As for reactions with the Sn(Cu) solders, as the compound thickness decreases, the Ni content in the Ni-*y*Co layers increases.

Key words: Interfacial reactions, Sn(Cu) solder

INTRODUCTION

Bond-pad metallization plays a critical role in creating reliable solder joints in electronic packaging.[1,2] In particular, when Pb-free solders are implemented in the near future, suitable bond-pad metallization will be very important for forming reliable solder joints. Currently, Cu-based bond pads are widely used in the various assembly technologies utilized in the field of electronic packaging. When Pb-free Sn-rich solders are reflowed with Cu-based bond pads, extensive reactions at the Sn-rich solder/Cu interface could occur, leading to vast interfacial Cu-Sn compound formation and serious Cu dissolution. This phenomenon at the interface would cause reliability issues, such as degradation of joint strength and electromigration (EM)-induced failure.[3] Therefore, Ni-based metal barrier layers, such as Ni(P) and electroplated Ni layers, are often used for Cu-based bond pads.[4,5] However, Ni(P) layers have been known to cause some serious reliability issues. One of these is the notorious “black-pad” issue. So, developing a suitable alternative metal layer to replace Ni(P) is still urgently needed to achieve sound and reliable Pb-free Sn-rich solder joints.

Co is a possible candidate to be used for the metal bond pad. Its use as a bond-pad metal has been studied and evaluated.[6,7] The advantages of using Co bond pads have been identified as: (1) superior wettability compared with the Ni(P) bond

(Received April 4, 2010; accepted July 30, 2010; published online September 1, 2010)

pad, and (2) solder/Co joints exhibit higher mechanical joint strength than that of solder/Ni(P) joints.[8] However, a fast reaction could occur between the Sn-based solders and Co metal layers. Vast intermetallic compound formation at the joint interface is not desired, and usually results in a low-strength solder joint. Adding Ni to the Co layer may possibly suppress the interfacial Sn/Co reaction. Yamamoto et al. have studied the interfacial reactions between Sn-Ag solder and Ni-20Co bond pads.[9] They found that the interfacial compound phase is the (Ni,Co)Sn_2 phase, rather than the common Ni_3Sn_4 phase that forms at the solder/Ni interface. In this present work, we investigated the feasibility of using Ni-Co alloys as bond pads for Pb-free solders. To that end, various compositions of Ni-Co alloy layers were prepared. The behavior of the interfacial reactions between Sn-based solders and the binary Ni-Co alloy layers was also systematically investigated. Sn(Cu) solders are the most common among the Pb-free solder candidates. Sn(Cu) solders with different Cu contents can be used to react with the metal bond pads of binary Ni-Co alloys.

EXPERIMENTAL PROCEDURES

Rectangular (1×0.5 cm^2) pieces of Cu foil were cut off from a Cu metal sheet (99.98% purity), purchased from Alfa Aesar Inc. The Cu foils were preground with sandpaper and finished using 1-μm alumina powder polishing. Then, the binary Ni-*y*Co alloy layers were electroplated onto the polished Cu foils. The compositions of the electroplated Ni-*y*Co layers were Ni, Ni-20Co, Ni-63Co, and Co (in at.%). Then, the electroplated Ni-*y*Co layers were ready for reflow with Sn(Cu) Pb-free solders. The studied compositions of the Sn(Cu) solders were Sn, Sn-0.2Cu, Sn-0.7Cu, and Sn-1.2Cu. The preparation of the Sn(Cu) solders was as follows: First the desired weight ratio of pure Sn and Sn-3Cu pieces were cut and then melted in flux ambient to produce Sn(Cu) alloys of different compositions. The Sn(Cu) alloys were cut and melted under flux ambient to produce spherical solder balls with a diameter of 400 μm. As shown in Fig. 1, Sn(Cu) solder balls were subsequently reflowed on prefluxed (resin mildly activated, RMA) electroplated Ni-*y*Co layers at a constant temperature of 250°C for various reflow times (10 s, 30 s, 60 s, and 300 s). After a certain reflow period, the reflowed Sn(Cu)/Ni-*y*Co samples were cleaned by alcohol using an ultrasonic machine. The cleaned samples were mounted with epoxy resin. Prior to scanning electron microscopic (SEM; Hitachi S3000H) cross-sectional study, the epoxy-mounted samples were first ground with sandpaper and finally polished with 0.3-μm alumina powder. Polished samples were then lightly etched with 5% HCl solution for 10 s to 15 s to delineate the morphology of the intermetallic compounds. Then, electron probe microanalysis (EPMA; JXA 8800M) was used to accurately determine the composition of the interfacial compound phases.

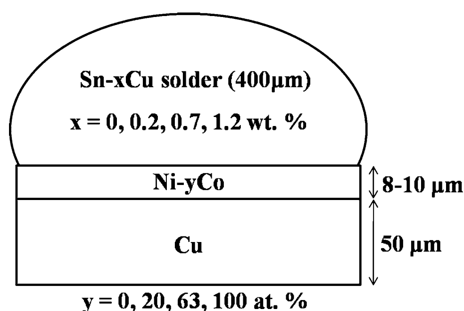

Fig. 1. Scheme of Sn-*x*(Cu)/Ni-*y*(Co)/Cu interfacial reactions.

RESULTS AND DISCUSSION

Interfacial Reactions Between Pure Sn and the Ni-*y*Co Layers

Figure 2 shows cross-sectional SEM images of the Sn/Ni-*y*Co samples after 30 s, 60 s, and 300 s of reflow. For the Sn/Ni samples, as seen in Fig. 2a1–a3, a Ni_3Sn_4 compound layer typically formed at the Sn/Ni interface. Figure 2b1–b3 shows the reactions at the Sn/Ni-20Co interfaces for different reflow times. After a short reflow of 30 s, a continuous ternary (Ni,Co)Sn_2 compound layer formed at the Sn/Ni-20Co interface. We believe that the (Ni,Co)Sn_2 reaction product has the same basic structure as the $CoSn_2$ phase, but dissolves with Ni atoms. After prolonged interfacial reactions (60 s and 300 s of reflow), the (Ni,Co)Sn_2 grew slightly at the interface. EPMA analysis identified the exact composition of the (Ni,Co)Sn_2 compound phase to be $(Ni_{0.72},Co_{0.28})Sn_2$.

From the above observations, three major points can be concluded: (1) the $CoSn_2$ phase is the first phase to form at the Sn/Ni-20Co interface;[10] (2) the Sn/Co reaction is more favorable than the Sn/Ni reaction at the Sn/Ni-20Co interface;[11–16] and (3) the Sn/Co reaction is the controlling step for the growth of the (Ni,Co)Sn_2 reaction product. Once the interfacial $CoSn_2$ phase formed at the Sn/Ni-20Co interface, Ni would be substituted for Co atoms in the $CoSn_2$ compound to form a ternary (Ni,Co)Sn_2 compound phase. The ternary Sn-Ni-Co phase diagram at 250°C (Fig. 3) shows that the Ni solubility in the (Ni,Co)Sn_2 phase can be as high as 96 at.%.[17] Ni atoms were extensively substituted for Co atoms in the $CoSn_2$ phase. In the final Sn/Ni-20Co case, EPMA analysis showed that 72 at.% of Co atomic sites were substituted with Ni atoms after 600 s of reflow. We believe the Ni percentage in the (Ni,Co)Sn_2 compound phase to be governed by the composition of the Ni-20Co substrate. This is why the actual Ni percentage (72 at.%) in the (Ni,Co)Sn_2 compound phase was lower than the maximum Ni solubility (96 at.%) as estimated from the ternary Sn-Ni-Co phase diagram.

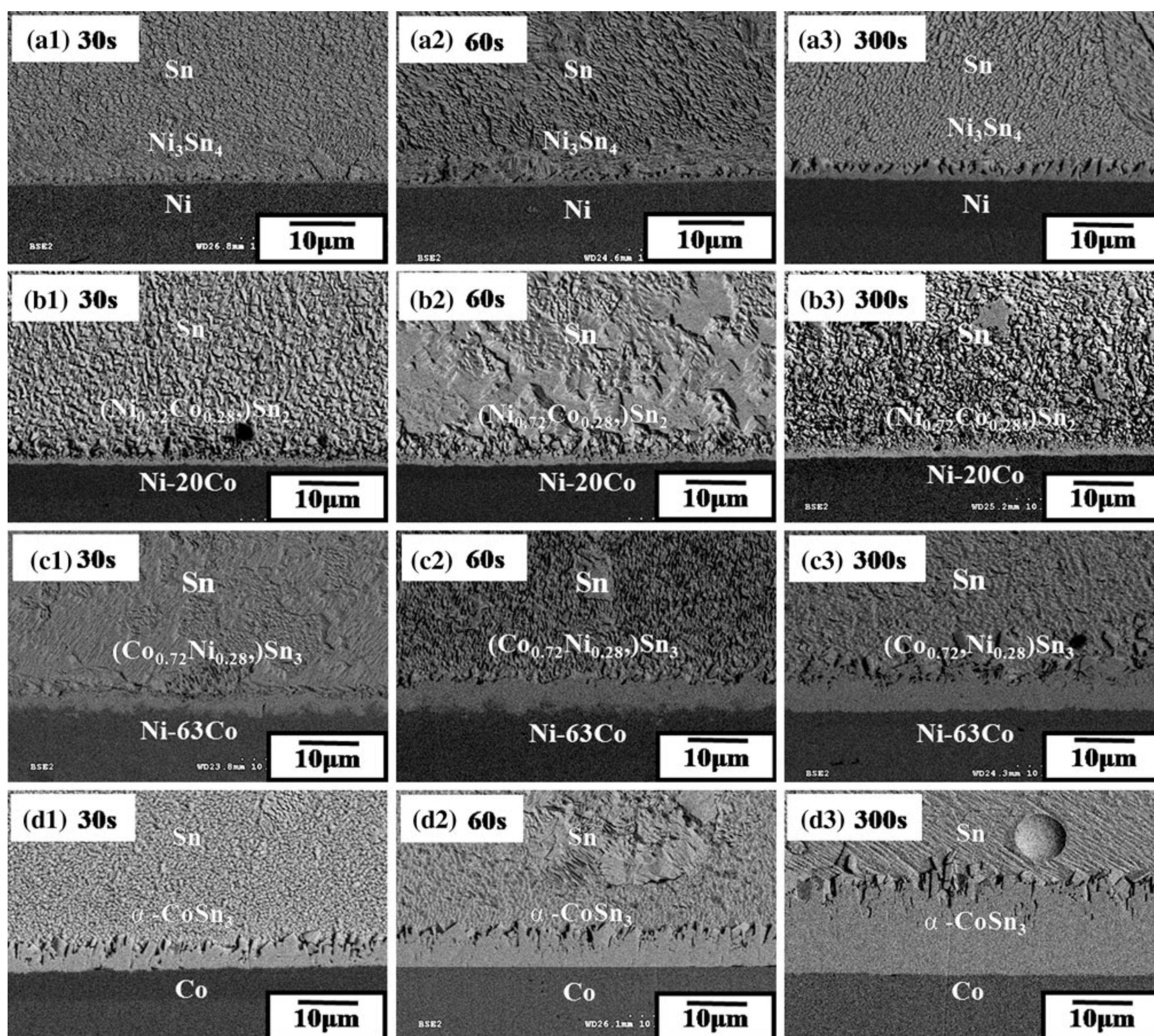

Fig. 2. SEM cross-sectional images of Sn/Ni-*y*Co (*y* = 0 at.%, 20 at.%, 63 at.%, 100 at.%) samples for different reflow times at 250°C.

As Sn reacts with the high-Co-containing Ni-63Co layer, as seen in Fig. 2c1–c3, the (Co,Ni)Sn_3 compound phase formed at the Sn/Ni-63Co interface. EPMA analysis shows that the composition of the (Co,Ni)Sn_3 phase can be determined to be ($Co_{0.72}$,$Ni_{0.28}$)Sn_3. We note that the percentage of Ni substitution (28 at.%) in the ($Co_{0.72}$,$Ni_{0.28}$)Sn_3 phase at the Sn/Ni-20Co interface is very close to the value predicted from the ternary Sn-Ni-Co phase diagram, which is about 31 at.%. Also, we found that the interfacial (Co,Ni)Sn_3 compound layer grew much faster than the (Co,Ni)Sn_2 phase at the Sn/Ni-20Co interface. Figure 2d1–d3 shows the interfacial reactions between Sn and the pure Co layer for different reflow times. Fast $CoSn_3$ layer formation was observed at the Sn/Co interface during the reflow process. The thickness of the interfacial compound layers at the Sn/Ni-*y*Co interfaces is plotted against the square root of reflow time in Fig. 4. When the Co concentration in the Ni-*y*Co layers was higher, the growth rate of the interfacial compound layer was faster. In addition, the relationship between the thickness of the interfacial compound layer and the square root of reflow time is quite linear. This linear relationship indicates that the growth mechanism of the interfacial compound layers is diffusion controlled. So, the kinetics of the growth of the interfacial compound at the Sn/Ni-*y*Co interfaces can be described by the following equation:

$$X = (Dt)^{1/2}, \quad (1)$$

where X is the average thickness of the interfacial compound layer, D is the diffusion coefficient, and t is the reflow time. From the above observations, we can identify that the Sn/Co reaction is favored

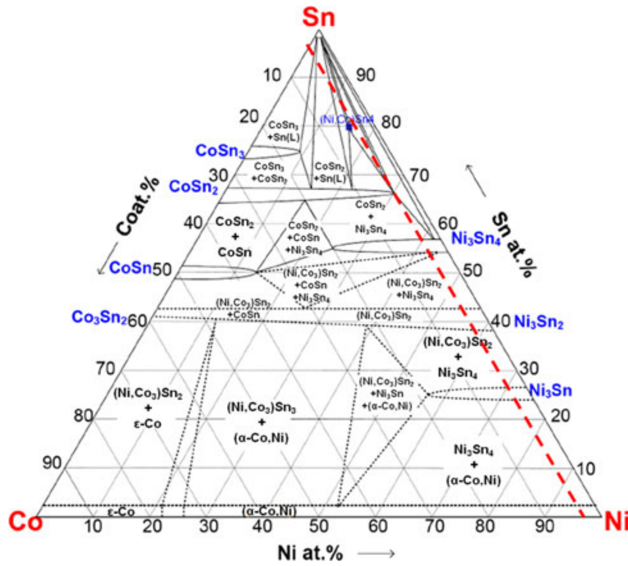

Fig. 3. Ni-Co-Sn ternary phase diagram at 250°C.[11]

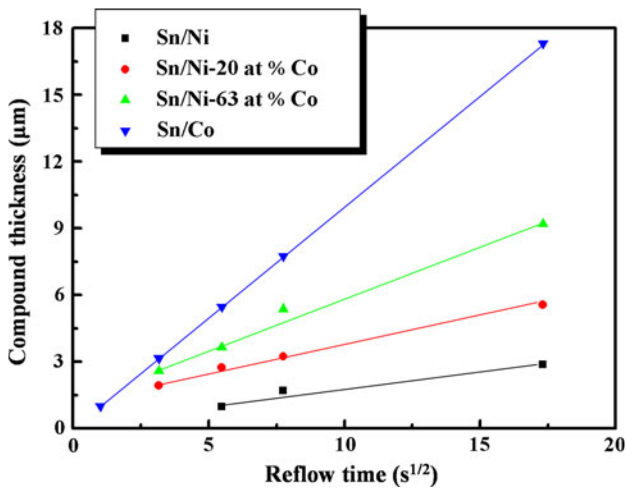

Fig. 4. Plot of the thickness of the interfacial compound layer versus the square root of reflow time for the Sn/Ni-*y*Co reaction.

over the Sn/Ni reaction, which dominates the interfacial reactions at the Sn/Ni-*y*Co interfaces. So, we believe that Co diffusion in the interfacial $(Ni,Co)Sn_2$, $(Co,Ni)Sn_3$ and $CoSn_3$ compound layers is the controlling process for the growth of the interfacial compound layers at the Sn/Ni-*y*Co interfaces. The slopes of the linear curves in Fig. 4 represent the Co diffusivities in the corresponding interfacial compound layers.

By using an acid solution (5% HNO_3 + 2% HCl + 93% methanol), the entire Sn solder ball on the interfacial compound layer can be etched away completely; the top morphology of the interfacial compound phases can then be observed. Figure 5a shows typically faceted Ni_3Sn_4 grains at the Sn/Ni interface. The top morphology of the interfacial $(Ni_{0.72},Co_{0.28})Sn_2$ compound phase at the Sn/Ni-20Co interface is shown in Fig. 5b, appearing to have hexagonal rod shapes, whereas the $(Co_{0.72}, Ni_{0.28})Sn_3$ and $CoSn_3$ compound phases at the Sn/Ni-63Co interface and the Sn/Co interface have a plate-like shape, as shown in Fig. 5c and d. With the dissolution of Ni, the $(Co,Ni)Sn_3$ plates become thicker than the $CoSn_3$ plates.

Interfacial Reaction Between Sn-*x*(Cu) and Ni-*y*Co Layers

Currently, Sn(Cu) is the most common Pb-free solder used in the electronics packaging industry.[18] Thus, it is of interest to study the interfacial reactions between Sn(Cu) solders and Ni-*y*Co bond-pad layers. Sn(Cu) solders with three different Cu contents were studied: 0.2 wt.%, 0.7 wt.%, and 1.2 wt.%. The interfacial reactions between Sn(Cu) and pure Ni have been reported on in many research works. When the Cu concentration was larger than 0.5 wt.%, only the $(Cu,Ni)_6Sn_5$ phase would be stable at the Sn(Cu)/Ni interface.[18] Figure 6 shows the results of the interfacial reactions between the Sn(Cu) solders and Co layers. $CoSn_3$ is the only interfacial compound phase formed at the Sn(Cu)/Co interfaces in spite of the Cu concentration. Also, we found that Cu additives in the Sn(Cu) solders slightly affected the growth rates of the interfacial $CoSn_3$ compound layers at the Sn(Cu)/Co interfaces. With higher Cu content in the Sn(Cu) solders, the growth rate of the interfacial compound layer would be slightly lower. Apparently, the Cu additive in Sn(Cu) solders had no influence on the interfacial compound phase formation and only a slight effect on the growth rate at the Sn(Cu)/Co interface.

Figure 7 shows the interfacial reactions between the Sn(Cu) solders and the Ni-63Co layers. Like the pure Sn/Ni-63Co case, the basal $CoSn_3$ phase formed at the Sn(Cu)/Ni-63Co interface. Cu, Ni, and Co have a very similar electronegativity and atomic radius.[19] So, both Ni and Cu can be substituted for Co in the interfacial $CoSn_3$ compound layer to form $(Co,Ni,Cu)Sn_3$ compound layers. We found that the Cu content in the Sn(Cu) solder had a greater influence on the interfacial compound formation. The growth rates of the interfacial $(Co,Ni,Cu)Sn_3$ compound layers at the Sn(Cu)/Ni-63Co interfaces decreased with the Cu content in the Sn(Cu) solders. The higher the Cu concentration in the Sn(Cu) solders, the slower the growth rate of the interfacial $(Co,Ni,Cu)Sn_3$ compound layer. The Cu additives in the Sn(Cu) solders clearly suppressed the growth rate of the interfacial $(Co,Ni,Cu)Sn_3$ compound layer.

Figure 8 shows the interfacial reactions between the Sn(Cu) solders and the Ni-20Co layers. Unlike the Sn(Cu)/Ni-63Co case, we found that the phase formed at the Sn(Cu)/Ni-20Co interfaces depended on: (1) the Cu content in the Sn(Cu) solders, and (2)

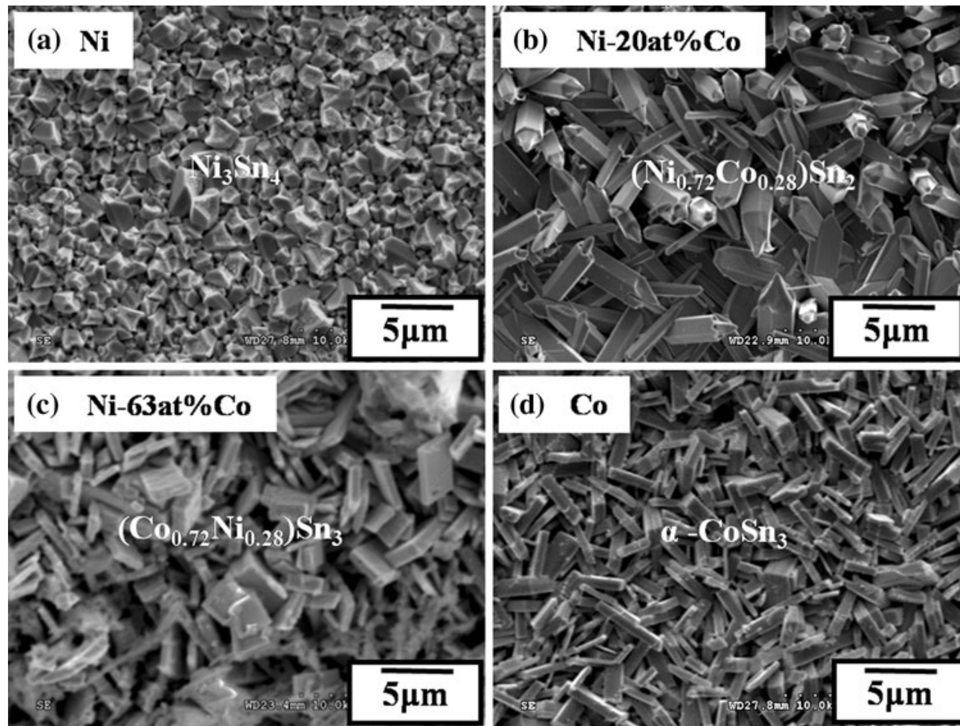

Fig. 5. Top-view images of the Sn/Ni-*x*Co interface after 250°C soldering for 300 s.

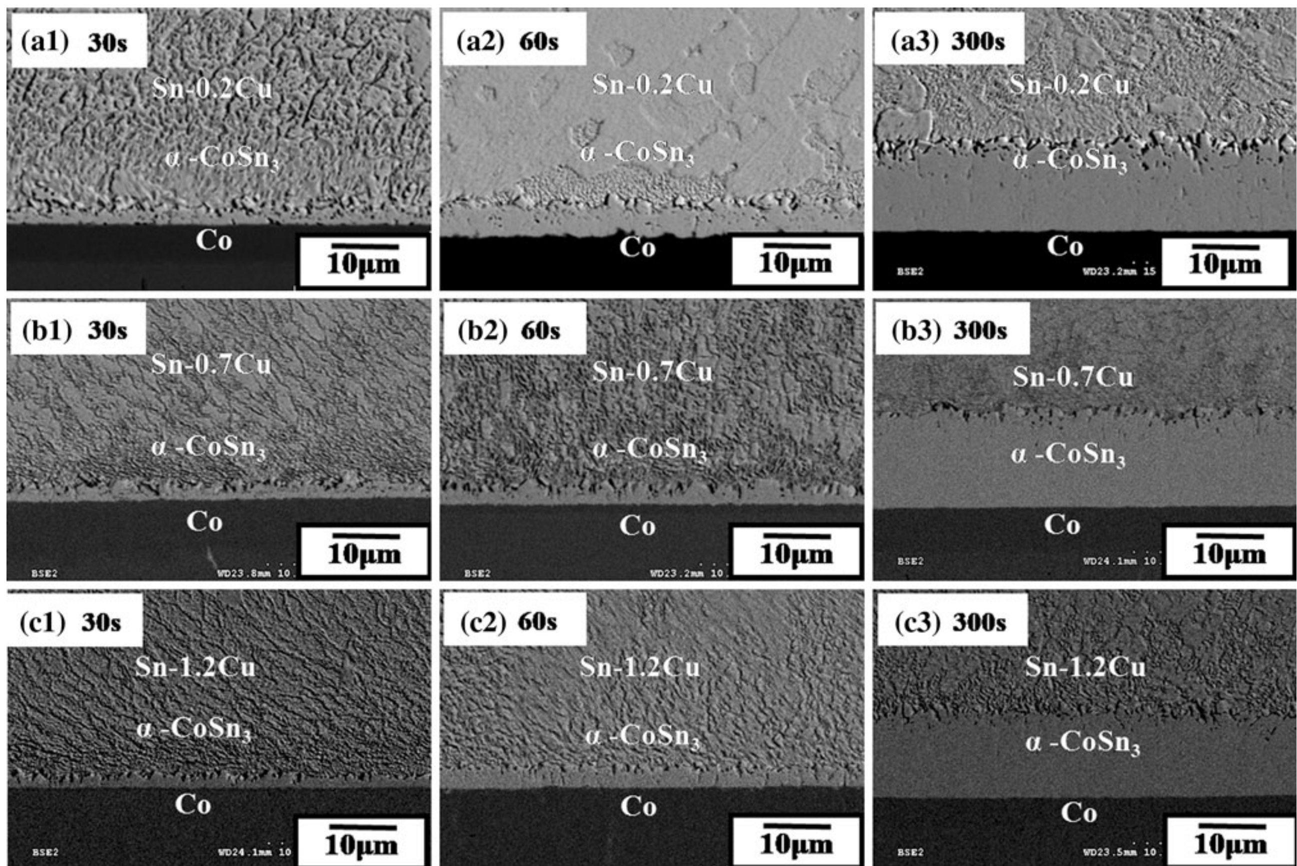

Fig. 6. SEM cross-sectional images of Sn-*x*Cu/Co (*x* = 0 wt.%, 0.2 wt.%, 0.7 wt.%, 1.2 wt.%) samples for different reflow times at 250°C.

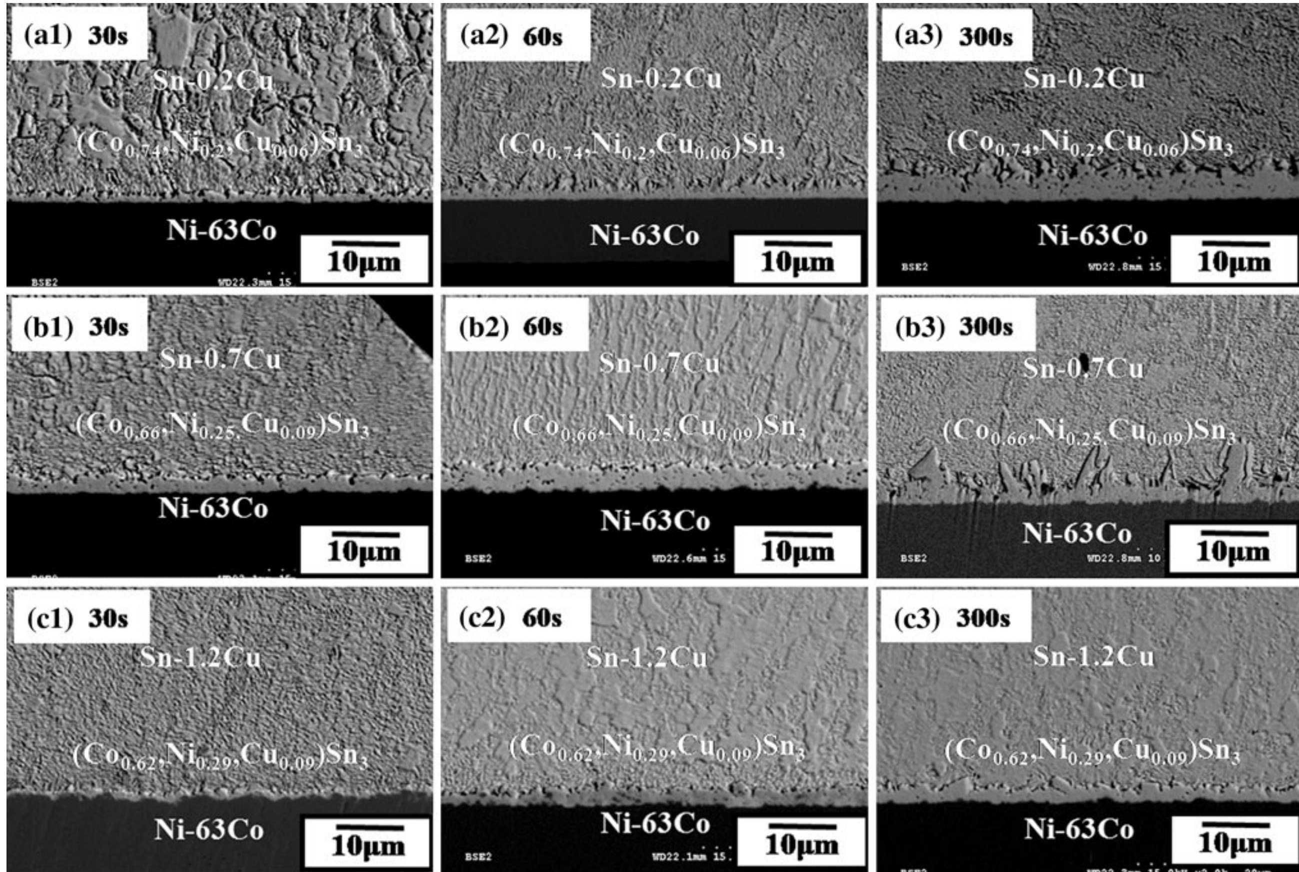

Fig. 7. SEM cross-sectional images of Sn-xCu/Ni-63 at.%Co (x = 0 wt.%, 0.2 wt.%, 0.7 wt.%, 1.2 wt.%) samples for different reflow times at 250°C.

the reflow time. In the case of low-Cu-content Sn(Cu) solders (Sn and Sn-0.2Cu), only a continuous $(Ni_x,Cu_y,Co_{1-x-y})Sn_2$ compound layer could be observed at the Sn(Cu)/Ni-20Co interface after up to 300 s of reflow. However, for the cases with high Cu content in the Sn(Cu) solders (Sn-0.7Cu and Sn-1.2Cu), the $(Ni_x,Cu_y,Co_{1-x-y})Sn_2$ compound layer formed early on, after 60 s of reflow. Then, after prolonged reflow (300 s), another needle-like interfacial $(Ni_x,Co_y,Cu_{1-x-y})_3Sn_4$ phase formed above the continuous $(Ni_x,Cu_y,Co_{1-x-y})Sn_2$ compound layer. The stoichiometry of the $(Ni_x,Co_y,Cu_{1-x-y})_3Sn_4$ phase does not match any of the Co-Sn compound phases in the binary Co-Ni system. Therefore, we believe that the basic structure of the interfacial $(Ni_x,Co_y,Cu_{1-x-y})_3Sn_4$ compound phase should belong to the structure of the Ni_3Sn_4 phase. Co and Cu are the solute atoms substituted for the Ni atoms in the $(Ni_x,Co_y,Cu_{1-x-y})_3Sn_4$ phase.

Growth Mechanism of the Interfacial $(Ni,Co)Sn_2$ Compound Layer

It has been pointed out previously that the Co-Sn reaction is the dominant reaction at the Sn(Cu)/Ni-yCo interfaces. Co in the outermost surface layer of the Ni-yCo layers would preferentially react with Sn in the Sn(Cu) solders. $CoSn_2$ or $CoSn_3$ would be the first basal phase formed at the Sn(Cu)/Ni-yCo interfaces. After an initial short reflow, Co atoms in the outermost surface layer of the Ni-yCo layers would be largely consumed. Thus, the Ni-yCo layers immediately beneath the interfacial $CoSn_2$ compound layer would be highly enriched with Ni. Ni and Co can mutually substitute for each other and form a complete Ni-Co solid solution. So, accompanied with the formation of the Co-Sn interfacial compound layer, Ni atoms in the enriched thin Ni-yCo layer near the Sn(Cu)/Ni-yCo interface would diffuse into the interfacial $CoSn_2$ or $CoSn_3$ compound layers to substitute for the Co atoms. We can conclude that the formation of the $(Ni_x,Cu_y,Co_{1-x-y})Sn_2$ compound layer relies on two in-series processes: (1) the formation of the interfacial Co-Sn compound layer, and (2) Ni dissolution into the interfacial Co-Sn compound layer.

From the ternary Sn-Ni-Co phase diagram in Fig. 3, we note that the maximum Ni substitution percentage for the Co atomic sites in the $(Ni_x,Co_y)Sn_2$ phase could be as high as 96 at.%. This means that, if there is sufficient Ni supply from the Ni-yCo substrate, theoretically, the Ni substitution percentage in the $(Ni_x,Co_y)Sn_2$ compound layer could reach 96 at.%. If the Ni percentage in the

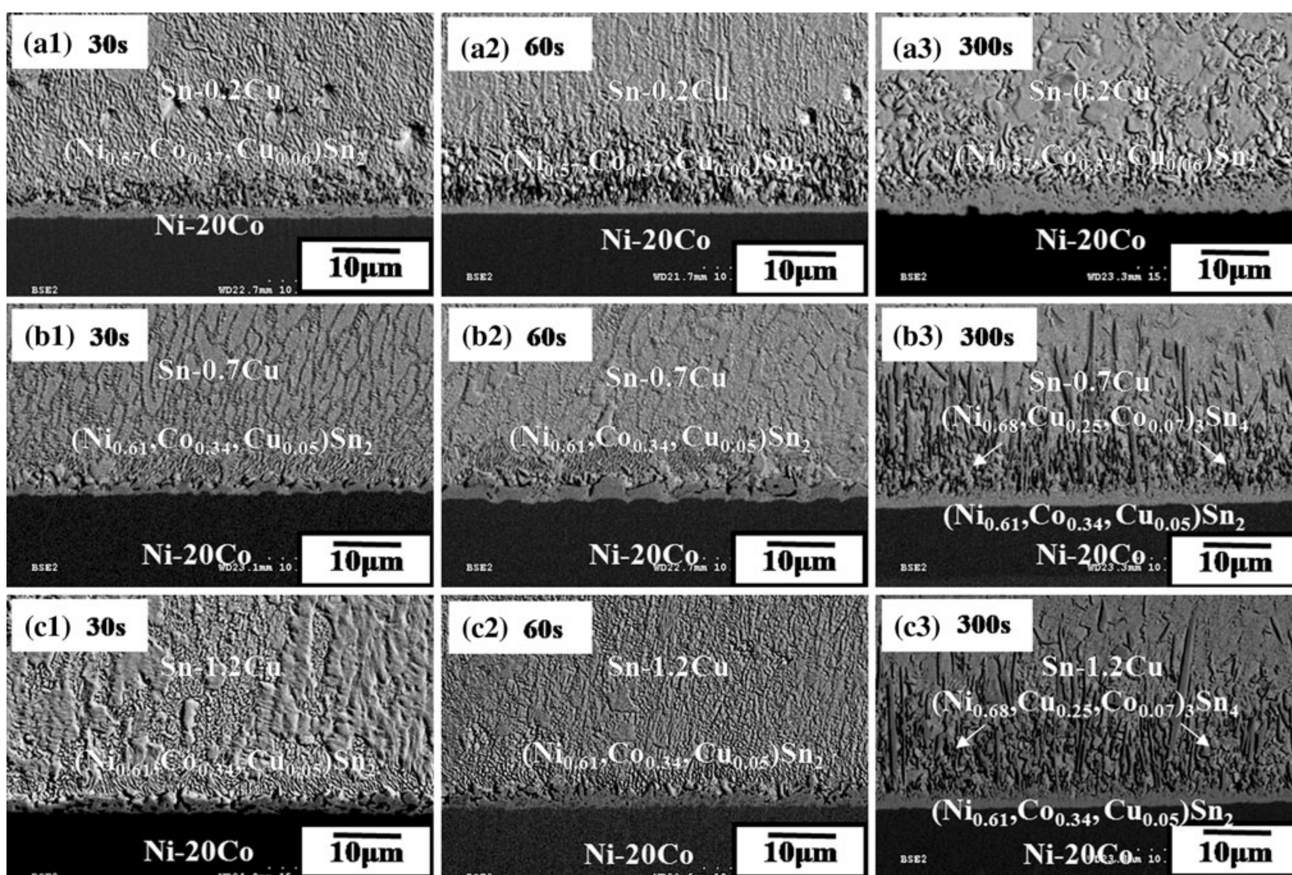

Fig. 8. SEM cross-sectional images of Sn-*x*Cu/Ni-20 at.%Co (*x* = 0 wt.%, 0.2 wt.%, 0.7 wt.%, 1.2 wt.%) samples for different reflow times at 250°C.

Ni-*y*Co substrate is <96 at.%, then the Ni substitution percentage in the $(Ni_x,Co_y)Sn_2$ compound layer would be limited by the Ni-to-Co atomic ratio in the Ni-*y*Co layers. Thus, the Ni-to-Co atomic ratio in the Ni-*y*Co layer would ultimately define the Ni substitution percentage in the interfacial $(Ni_x,Co_y,Cu_{1-x-y})Sn_2$ compound layer. The above findings can be verified by looking at Table I, which lists the exact composition of the interfacial compound layer at the Sn(Cu)/Ni-*y*Co interfaces as determined by EPMA. For example, in the current Ni-20Co case, the maximum Ni substitution percentage in the interfacial $(Ni_x,Cu_{1-x})Sn_2$ compound would be no more than 80 at.%. In addition, we note that the Ni substitution percentage in the $(Ni_x,Cu_y,Co_{1-x-y})Sn_2$ compound layer at the Sn/Ni-20Co interface is reduced from 72 at.% to around 60 at.% in the Sn-0.2Cu/Ni-20Co case. These findings imply that the presence of Cu in the Sn(Cu) solders would lead to a reduction in the Ni substitution percentage in the $(Ni_x,Cu_y,Co_{1-x-y})Sn_2$ compound layer.

Figure 9 shows the interfacial compound thickness versus the Ni content in the Ni-*y*Co layers that have reacted with Sn(Cu) solders after 300 s of reflow time at 250°C. For the pure Sn solders, the thickness of the compound layer monotonically decreases with the Ni content in the Ni-*y*Co layers. We found that the compound thickness decreases almost linearly with the Ni content in the Ni-*y*Co layers. For the Sn(Cu) solders, the thickness of the compound layer also decreases with the Ni content in the Ni-*y*Co layers, but the decrease in the compound thickness of the Sn(Cu) solders is faster than that in the pure Sn case, as the Ni content in the Ni-*y*Co layers increases.

CONCLUSIONS

The interfacial reactions between electroplated Ni-*y*Co alloy layers and Sn(Cu) solders have been studied at a temperature of 250°C. We can conclude that the Co-Sn reaction is the dominant reaction in the Sn(Cu)/Ni-*y*Co reactions. (1) For pure Co layers, $CoSn_3$ is the only interfacial compound phase formed at the Sn(Cu)/Co interfaces in spite of the Cu concentration. Also, the Cu additive in Sn(Cu) solders does not have an obvious influence on the $CoSn_3$ compound growth at the Sn(Cu)/Co interfaces. (2) For the Ni-63Co layer, $(Co,Ni,Cu)Sn_3$ is the only interfacial compound phase formed at the Sn(Cu)/Ni-63Co interfaces. Unlike the pure Co layer case, the Cu additives in the Sn(Cu) solders clearly suppress the growth rate of the interfacial $(Co,Ni,Cu)Sn_3$ compound layer. (3) For the Ni-20Co

Table I. Summary of the exact composition of the interfacial compound layer at the Sn(Cu)/Ni-*y*Co interfaces as determined by EPMA

Solder	UBM	IMC Phase
Sn	Ni	Ni_3Sn_4[a]
	Ni-20 at.%Co	$(Ni_{0.72},Co_{0.28})Sn_2$
	Ni-63 at.%Co	$(Co_{0.72},Ni_{0.28})Sn_3$
	Co	$CoSn_3$
Sn-0.2Cu	Ni	$(Ni,Cu)_3Sn_4$[a]
	Ni-20 at.%Co	$(Ni_{0.57},Co_{0.37}, Cu_{0.06})Sn_2$
	Ni-63 at.%Co	$(Co_{0.74},Ni_{0.2},Cu_{0.06})Sn_3$
	Co	$(Co_{0.93},Cu_{0.07})Sn_3$
Sn-0.7Cu	Ni	$(Ni,Cu)_6Sn_5$[a]
	Ni-20 at.%Co	$(Ni_{0.61},Co_{0.34}, xCu_{0.05})Sn_2 + (Ni_{0.68},Cu_{0.25},Co_{0.07})_3Sn_4$
	Ni-63 at.%Co	$(Co_{0.66},Ni_{0.25},Cu_{0.09})Sn_3$
	Co	$(Co_{0.92},Cu_{0.08})Sn_3$
Sn-1.2Cu	Ni	$(Ni,Cu)_6Sn_5$[a]
	Ni-20 at.%Co	$(Ni_{0.64},Co_{0.33},Cu_{0.03})Sn_2 + (Ni_{0.68},Cu_{0.25},Co_{0.07})_3Sn_4$
	Ni-63 at.%Co	$(Co_{0.62},Ni_{0.29},Cu_{0.09})Sn_3$
	Co	$(Co_{0.89},Cu_{0.11})Sn_3$

[a]Results for Sn(Cu)/Ni from Ref. 12.

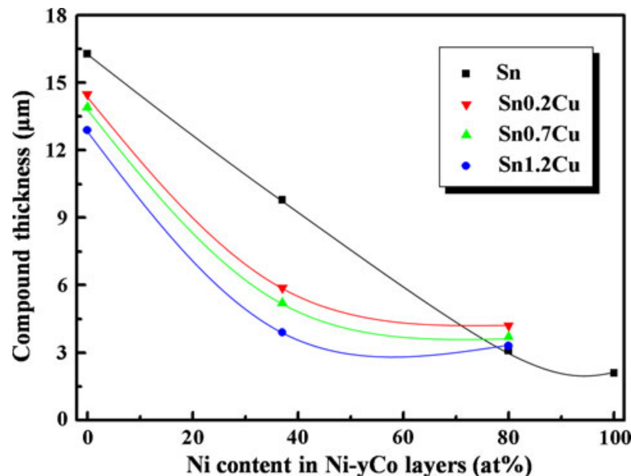

Fig. 9. Interfacial compound thickness versus the Ni content in the Ni-*y*Co layers reacting with Sn(Cu) solders after 300 s of reflow time at 250°C.

layer, the interfacial compound formation at the Sn(Cu)/Ni-20Co interfaces depends on the Cu content in the Sn(Cu) solders and the reflow time. For cases with high Cu content in the Sn(Cu) solders (Sn-0.7Cu and Sn-1.2Cu), additional needle-like interfacial $(Ni_x,Co_y,Cu_{1-x-y})_3Sn_4$ phases form above the continuous $(Ni_x,Cu_y,Co_{1-x-y})Sn_2$ compound layer.

The Ni content in the Ni-*y*Co layer can indeed reduce the interfacial compound formation at the Sn(Cu)/Ni-*y*Co interfaces. For pure Sn solders, the thickness of the compound layer monotonically decreases with the Ni content in the Ni-*y*Co layers. As it reacts with the Sn(Cu) solders, the decrease in the compound thickness is faster, as the Ni content in the Ni-*y*Co layers increases.

ACKNOWLEDGEMENTS

The authors would like to thank Professor J.G. Duh and Ms. S.Y. Tsai, from the Department of Materials Science and Engineering, Nation Tsing Hua University, for their help with the EPMA. The work was financially supported by the National Science Council (NSC), Taiwan.

REFERENCES

1. J.W. Nah and K.W. Paik, *IEEE Trans. Compon. Packag. Technol.* 25, 1 (2002).
2. C.K. Hu and J.M.E. Harper, *Mater. Chem. Phys.* 52, 5 (1998).
3. K. Zeng, R. Stierman, T.C. Chiu, and D. Edwards, *J. Appl. Phys.* 97, 024508 (2005).
4. H.S. Chun, J.W. Yoon, and S.B. Jung, *J. Alloys Compd.* 439, 91 (2007).
5. M. He, Z. Chen, and G. Qi, *Acta Mater.* 52, 2047 (2004).
6. R. Labie, E. Beyne, and P. Ratchev, *Proceedings of the 53rd Electronic Components Technology Conference* (Singapore: ECTC, 2003), pp. 1230–1234.
7. R. Labie, P. Ratchev, and E. Beyne, *Proceedings of the 55th Electronic Components Technology Conference* (Florida: ECTC, 2005), pp. 449–451.
8. L. Magagnin, V. Sirtori, S. Seregni, A. Origo, and P.L. Cavallotti, *Electrochim. Acta* 50, 4621 (2005).
9. T. Yamamoto, S. Sakatani, S. Kobayashi, K. Uenishi, K.F. Kobayashi, M. Ishio, K. Shiomi, A. Hashimoto, and M. Yamamoto, *Mater. Trans.* 46, 2406 (2005).
10. C.C. Chen and Y.T. Chan, *Intermetallics* 18, 649 (2010).
11. S. Bader, W. Gust, and H. Hieber, *Acta Mater.* 43, 329 (1994).
12. C.P. Huang, C. Chen, C.Y. Liu, S.S. Lin, and K.H. Chen, *J. Mater. Res.* 20, 2772 (2005).
13. Y.C. Lin and J.G. Duh, *Scripta Mater.* 54, 1661 (2006).

14. W.J. Zhu, J. Wang, H.S. Liu, Z.P. Jin, and W.P. Gong, *Mater. Sci. Eng. A* 456, 109 (2007).
15. C.H. Wang and S.W. Chen, *Intermetallics* 16, 524 (2008).
16. Y. Takashi, S. Shigeaki, K. Shinji, U. Keisuke, K. Kojiro, I. Masaaki, S. Kazuhiro, H. Akio, and Y. Masaharu, *Mater. Trans.* 46, 2406 (2005).
17. Y.H. Chao, S.W. Chen, C.H. Chang, and C.C. Chen, *Metall. Mater. Trans.* 39, 477 (2008).
18. C.E. Ho, S.C. Yang, and C.R. Kao, *J. Mater. Sci.* 18, 155 (2007).
19. I.E. Anderson and J.L. Harringa, *J. Electron. Mater.* 35, 94 (2006).